Supplementary Information: Nitrogen and boron co-doped carbon nanotubes embedded with nickel nanoparticles as highly efficient electromagnetic wave absorbing materials

Xin Zhu[a](朱鑫), Feng Yan[a*](闫峰), Chunyan Li[a](李春燕), Lihong Qi[a](齐立红), Haoran Yuan[a](袁浩然), Yanfeng Liu[b](刘岩峰), Chunling Zhu[b*](朱春玲), Yujin Chen[a,b,c*](陈玉金)

[a] Key Laboratory of In-Fiber Integrated Optics, Ministry of Education and College of Science, Harbin Engineering University, Harbin 150001, China

[b] College of Materials Science and Chemical Engineering, Harbin Engineering University, Harbin 150001, China

[c] School of Materials Science and Engineering, Zhengzhou University, Zhengzhou 450001, China

*Corresponding authors: Email: chenyujin@hrbeu.edu.cn; yanfeng@hrbeu.edu.cn; zhuchunling@hrbeu.edu.cn.

EXPERIMETNAL SECTION

Synthesis of nickel boride. 0.0475 g of nickel chloride hexahydrate(NiCl2•6H2O) and 0.2 g of polyvinylpyrrolidone(Polyvinylpyrrolidone，Mw=55000）were put into a three-necked round-bottom flask, and then add 5ml of deionized water to the flask, stir for one hour, and continue to pass in Ar during the process. Then, 0.025 g $NaBH_4$ dissolved into 20 ml of deionized water was quickly added to the flask with a syringe, and the solution immediately turned black. Finally, the black precipitate was filtered and washed with deionized water several times, and freeze-dried to obtain nickel boride black powder.

Synthesis of Ni@BNCNT. The nickel boride powder and dicyandiamide were put into the porcelain boat at a ratio of 1:30, and heated to a certain temperature at a rate of 5 ℃/min under argon flow for 2 hour.

Synthesis of $Ni(OH)_2$. 1.83 g of nickel nitrate and 0.8 g of sodium hydroxide were added to a beaker containing 200 mL of deionized water. Then the light green precipitate was obtained. The precipitate was washed with water, and then centrifuged and dried at 40^{o}C.

Synthesis of Ni@NCNT. The preparation of Ni@NCNT was similar to that Ni@BNCNT except that the nickel boride was replaced with $Ni(OH)_2$. The annealing temperature was set to 800 ^oC.

Characterizations. The morphology and size of the synthesized samples were characterized by X-ray powder diffraction (XRD) using a X Pert Pro diffractometer with Cu Kα radiation (λ=1.5418 Å). The structures of the samples were analyzed by scanning electron microscope (SEM, SU70, Hitachi) and transmission electron microscopy (TEM, JEM-2100F, JEOL) with an emission voltage of 200 kV. Sample surface element analysis were taken on X-ray photoelectron spectrometer (KAlpha,Thermofisher Scienticfic Company) with Al Kα radiation generated at 12 kV and 150 W. Raman spectrometer was used to test the degree of graphitization of carbon nanotube on Lab RAM Aramis micro Raman spectrometer with an excitation wavelength at 488 nm. The chemical composition of the samples was determined by inductively coupled plasma-optical emission spectroscopy (ICP-OES, Optima 8000 PE). The magnetostatic properties of Ni@BNCNT and Ni@NCNT were measured at room temperature by a vibrating sample magnetometer (VSM, 7410 series, Lake Shore).

Calculations for the differential charge density. By using the Material studios (MS) software to establish the crystal structure model, find the initial structure model of the graphite layer in the MS software, doping with boron and nitrogen elements. The formula for differential charge density is:

$$\Delta\rho=\rho_{AB}-\rho_A-\rho_B \quad (S1)$$

In the formula, ρ_{AB} represents the charge density of several materials after bonding, ρ_A and ρ_B represent the individual charge density of A and B in the material, respectively. Based on density functional theory (DFT), this paper uses VASP (Vienna Ab-initio Simulation Package) software, one of the first-principles calculation codes, calculated the charge distribution of Ni and C atoms at the interface between Ni NPs and BNCNT. When calculating, set the plane wave cut-off energy E-cut to 400 eV and K-point to 1*1*1.

Electromagnetic parameter measurements. The electromagnetic wave absorption

parameters of the material, namely the relative complex permittivity and the relative complex permeability, are tested by using a vector network analyzer (model Anritsu MS4644A Vectorstar). Before testing, we need to calibrate the instrument: short circuit-open circuit-load-through, and then use the coaxial method to scan the sample in the frequency range of 2-18 GHz. The sample and the paraffin matrix are uniformly mixed according to a certain filler ratio, and the mixture is pressed into a cylindrical shape with an inner diameter of 3.0 mm, an outer diameter of 7.0 mm, and a thickness of 2 to 3 mm, then measure its electromagnetic parameters.

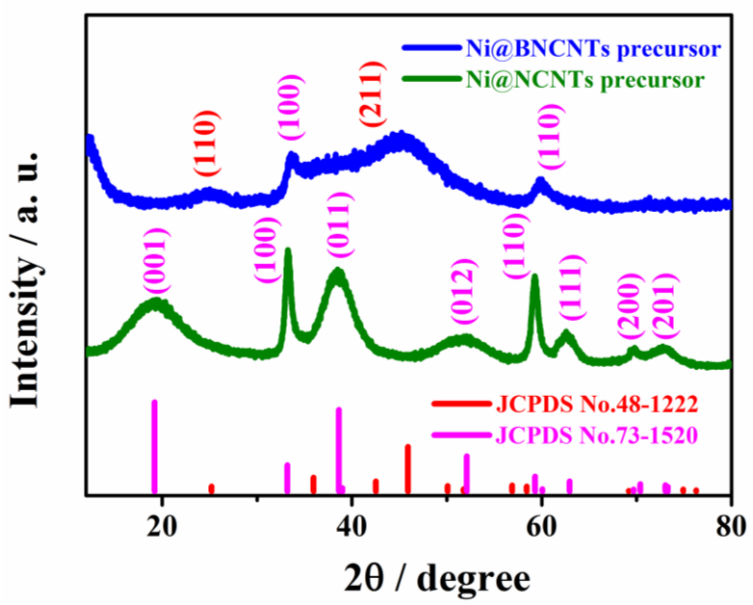

FIG. S1: XRD patterns of the precursors for Ni@BNCNTs and Ni@NCNTs.

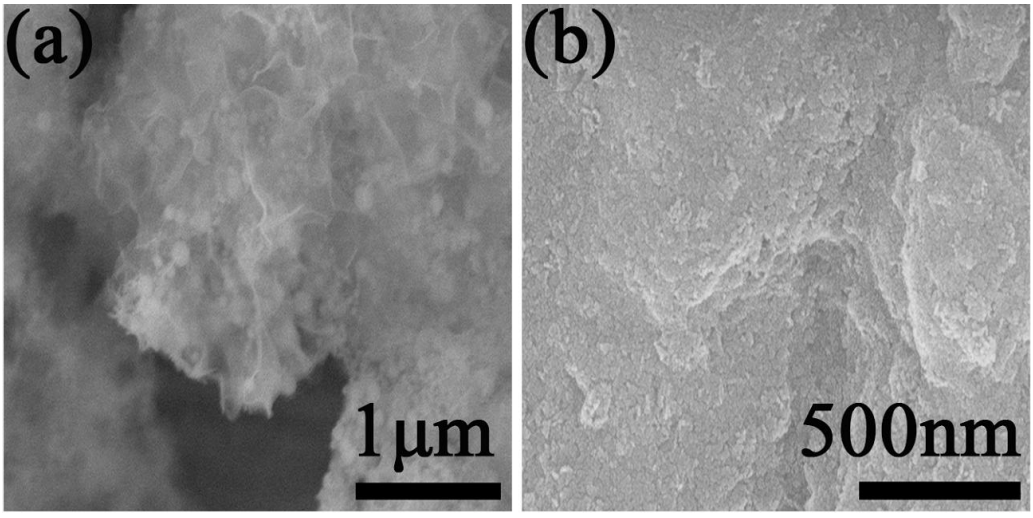

FIG. S2: SEM images of the precursor for (a) Ni@BNCNTs, and for (b) Ni@NCNTs.

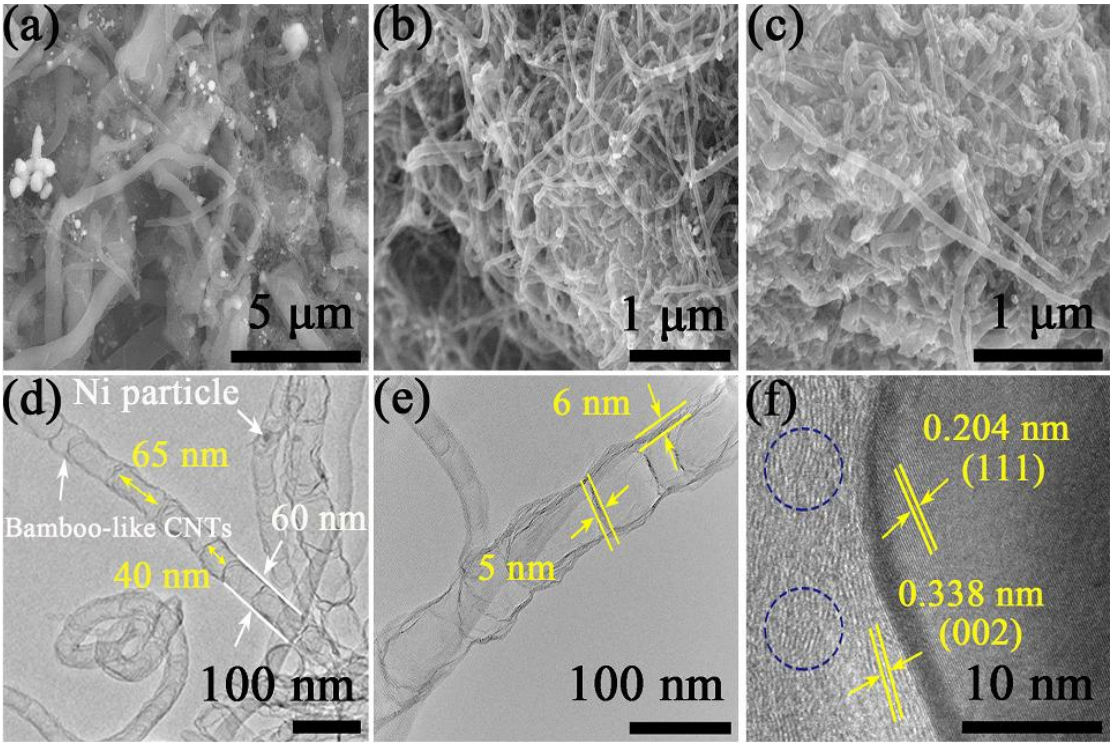

FIG. S3: SEM and TEM images of (a,d) Ni@NCNT-800, b,e) Ni@BNCNT-700, and (c,f) Ni@BNCNT-900.

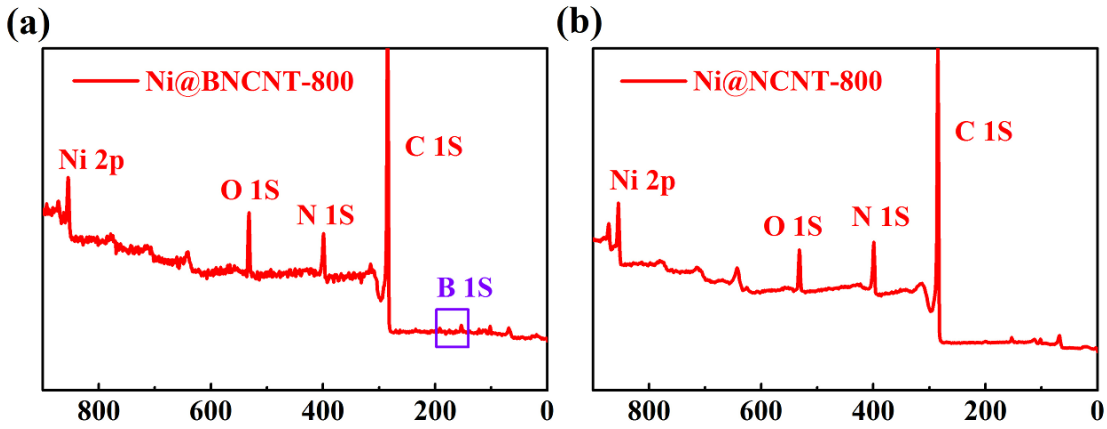

FIG. S4: The XPS survey spectrum of (a) Ni@BNCNT-800 and (b) Ni@NCNT-800.

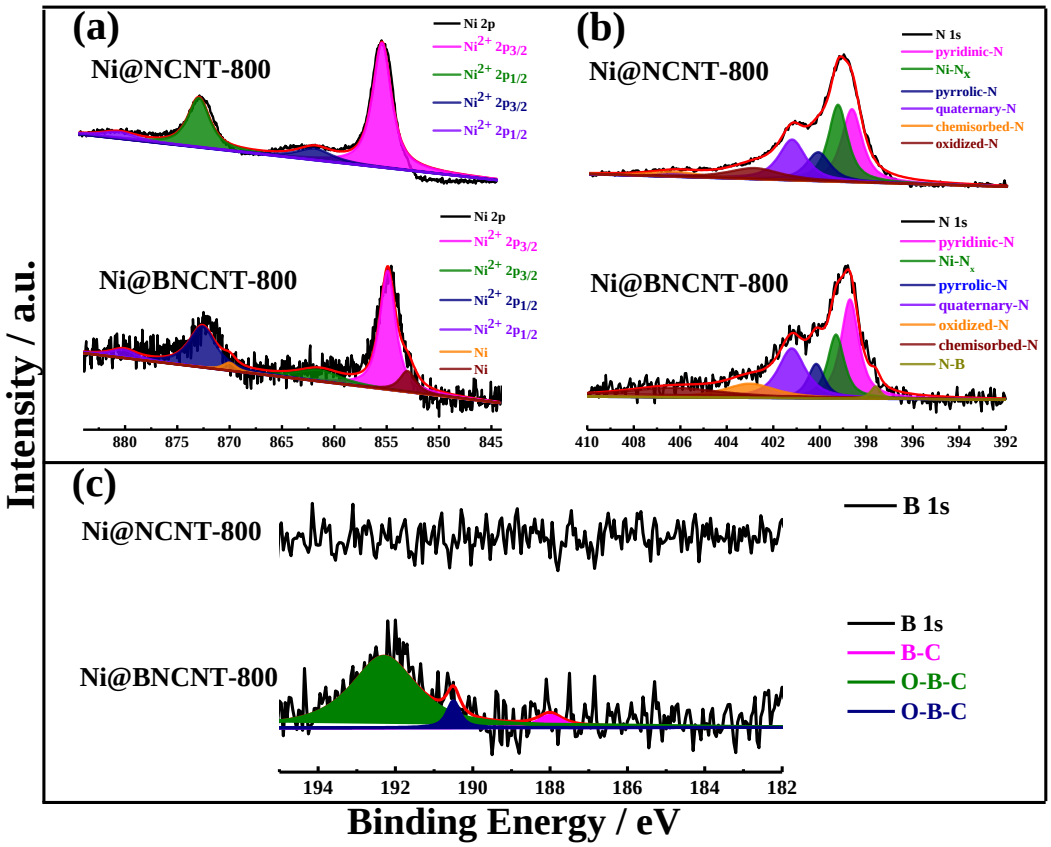

FIG. S5: (a) Ni 2p XPS spectra, (b) N 1s core-level XPS spectra, (c) B 1s core-level XPS spectra.

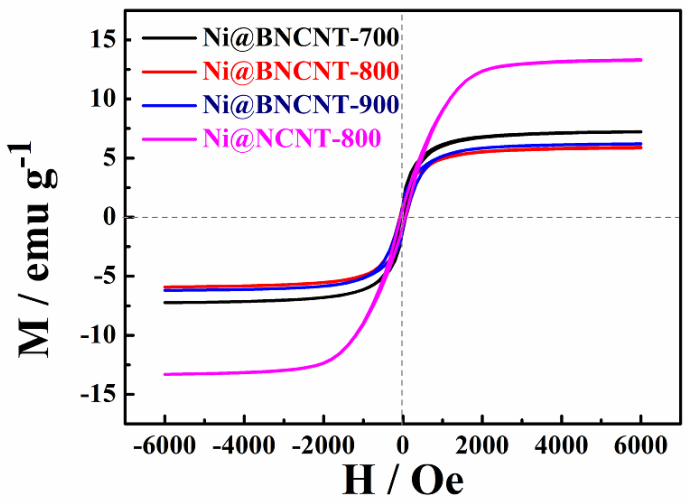

FIG. S6: Magnetization hysteresis loops of Ni@BNCNTs and Ni@NCNT-800.

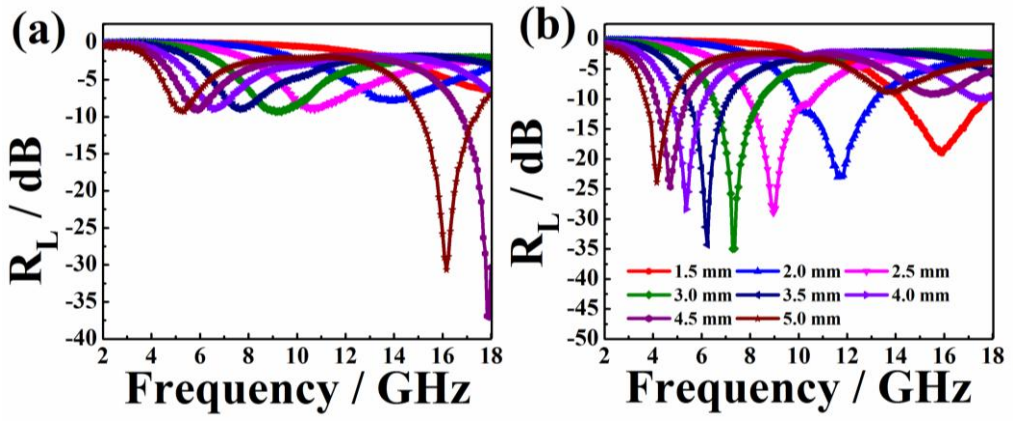

FIG. S7: Frequency-dependent R_L plots of (a) Ni@BNCNT-700 and (b) Ni@BNCNT-900 at d in range of 1.5 – 5.0 mm.

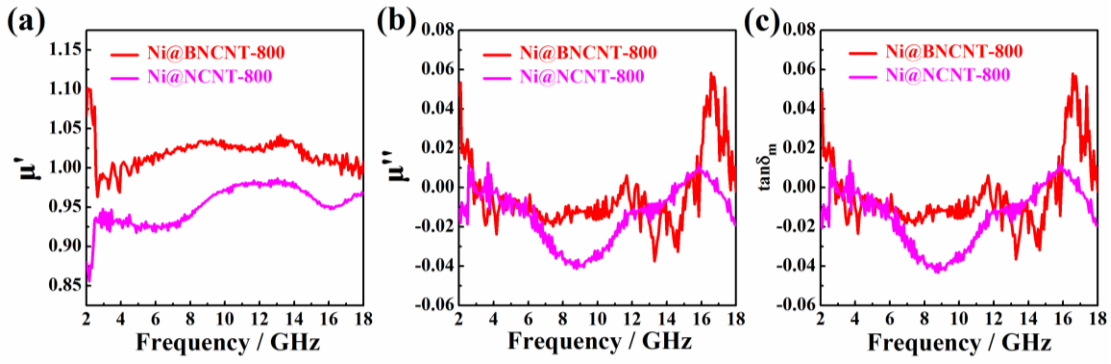

FIG. S8: (a) The real parts of the the complex permeabilities, (b) the imaginary parts of the complex permeabilities, and (c) the magnetic loss tangents of Ni@BNCNT-800 and Ni@NCNT-800.

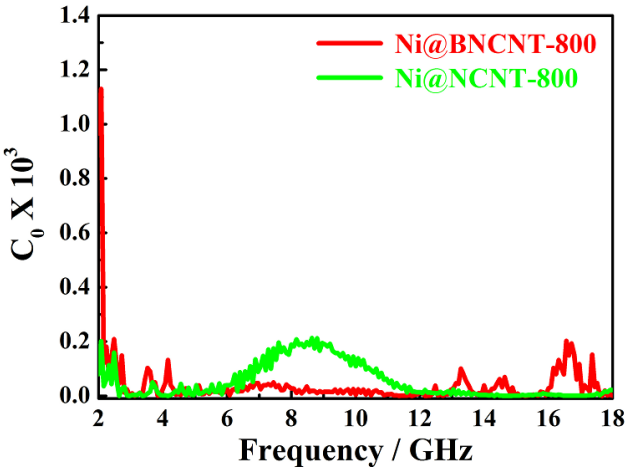

FIG. S9: $C_0 - f$ curves of Ni@BNCNT-800 and Ni@NCNT-800.

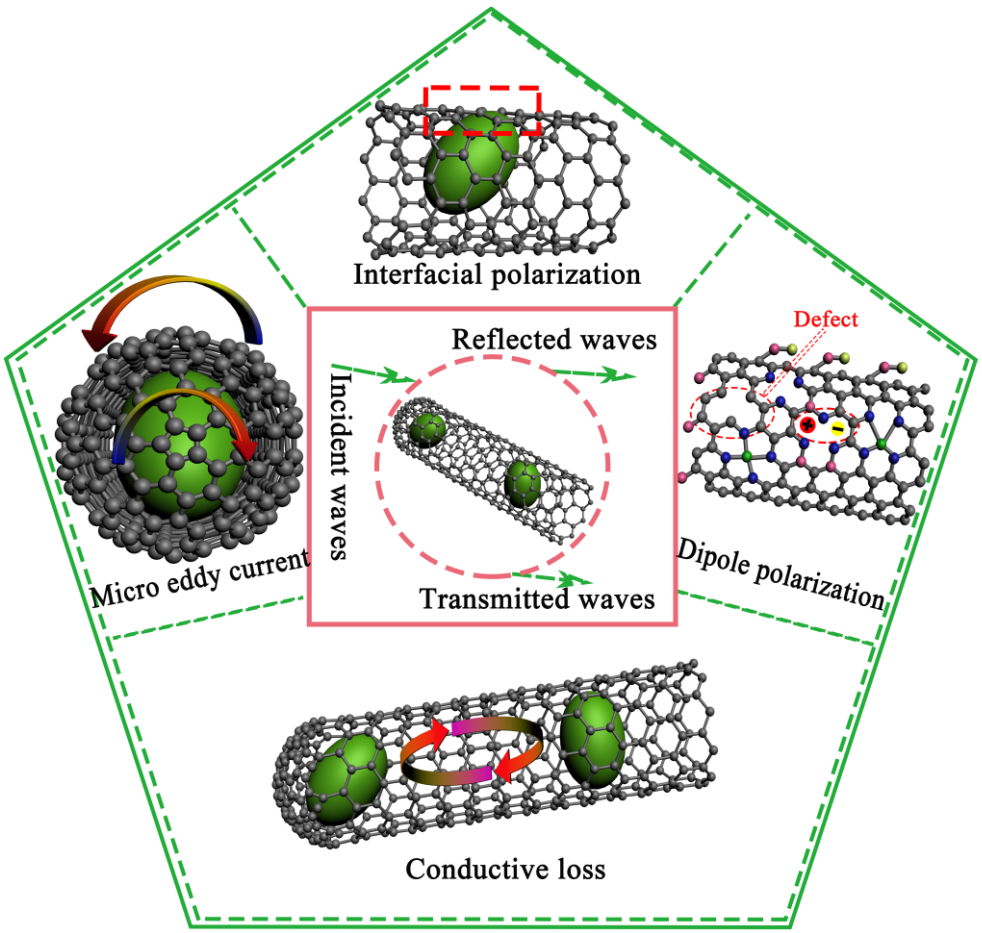

FIG. S10: Schematic illustration of the absorption mechanism for Ni@BNCNTs.

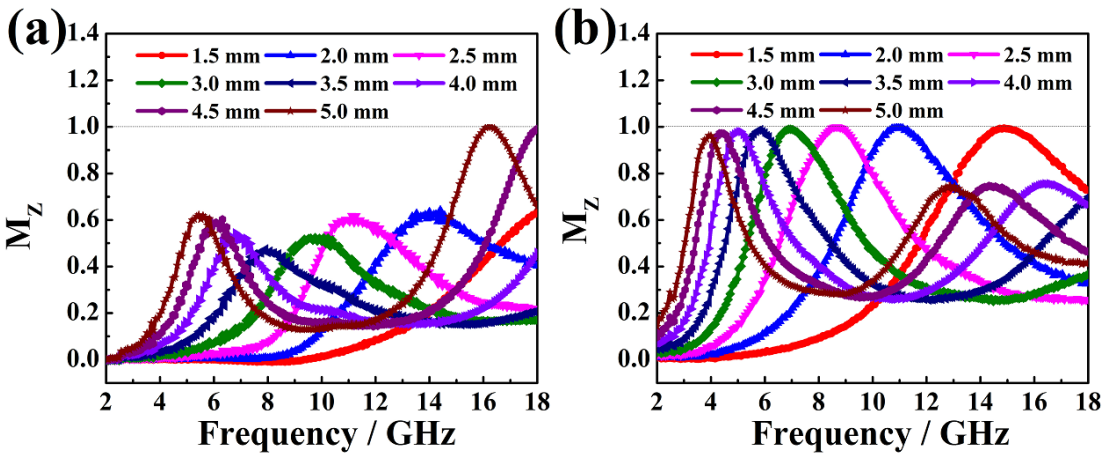

FIG. S11: M_Z-f plots of (a) Ni@NCNT-800 and (b) Ni@BNCNT-800.

Table S1 Comparison of EMW absorption properties of Ni@BNCNTs with those of the reported materials.

Samples	R_{Lmin} / dB	Thickness / mm	Filler rato / wt%	Ref.
Fe@CNTs	-22.7	3.5	20	7
MWCNT/CI	-16.9	1.5	50	8
Fe3O4/CNT (FCC14)	-43	1.5	30	9
CoNi/N-GCT	-41.1	3.5	25	14
Fe/NCNTs	-30.4	3.5	30	15
CoNi@NCNT	-49.8	3.5	20	16
Co/N-doped carbon nanofibers	-25.7	2.0	5	38
FeCo@C	-29	5	50	39
GO/CNT-Fe_3O_4	-37	5.0	30	40
Fe_3O_4/CNT	-25	5	88	41
CNTs/Ni	-22.89	5.0	30	10
Ni@C nanocapsules	-32	2.0	50	42
MoS_2 NS/U-NCNTs	-20.9	2.5	30	11
Fe_3O_4/carbon core/shell nanorods	-27.9	2.0	55	43
CoNi/GN	-30.1	2.0	60	44
Ni@BNCNTs	-37.5	2.5	25	This work

Table S2. The parameters of the samples according to H-N simulation.

Samples	α	β	t	σ_{fit}/S m^{-1}
Ni@BNCNT-700	0.67	0.96	0.14	0.05
Ni@BNCNT-800	0.31	0.9	0.49	0.24
Ni@BNCNT-900	0.54	1.0	0.30	0.12
Ni@NCNT-800	0.03	0.3	0.10	0.03